Relation between phase composition and photocatalytic activity of TiO_2 in a sulfoxide deoxygenation reaction.

Alessandra Molinari,[a*] Francesca Bonino,[b] Giuliana Magnacca,[b] Francesca Demaria,[a] Andrea Maldotti[a]

[a] *Dipartimento di Scienze Chimiche e Farmaceutiche, Università di Ferrara, Via Fossato di Mortara 17, 44121 Ferrara, Italy. Tel: +39 0532455378, Fax: +39 0532240709, alessandra.molinari@unife.it*
[b] *Dipartimento di Chimica, NIS and INSTM Reference Centre, Università di Torino, Via G. Quarello 15, I-10135 and Via P. Giuria 7, I-10125, Turin, Italy*

Abstract In the present study we synthesize three TiO_2 samples, TiO_2-500, TiO_2-750 and TiO_2-850, by a sol-gel procedure varying the rutile and anatase content by calcination at different temperatures. Characterization by XRD, NIR-Raman, UV-Raman, BET, DR-UV-Vis spectroscopy and SEM points out that TiO_2-500 consists mainly of anatase and TiO_2-850 of rutile. TiO_2-700 presents both phases on the surface that is the part of the photocatalyst interested by UV illumination. The photocatalysts are tested in the deoxygenation reaction of methyl p-tolyl sulfoxide to the corresponding sulfide using 2-propanol as hole scavenger. It is demonstrated that the presence of both anatase and rutile on the surface of TiO_2-700 is responsible of the increase of the photocatalytic activity. This is likely due to a more efficient charge separation process that increases lifetime of the charges giving availability of electrons and holes for the photocatalytic reaction. Methyl p-tolyl sulfide is formed with a selectivity of 100%.

Keywords: semiconductors, X-ray diffraction topography, Raman spectroscopy and scattering, irradiation effects, sulfoxide deoxygenation.

1. Introduction

Titanium dioxide (TiO_2) has been widely studied in photocatalysis from the beginning of 70s. Photoexcitation of this semiconductor yields holes in its valence band (h_{vb}^+) and electrons in its conduction band (e_{cb}^-) according to Eq. 1.

$$TiO_2 + h\nu \longrightarrow h_{vb}^+ + e_{cb}^- \qquad (1)$$

The two main kinds of crystalline TiO_2, anatase and rutile, exhibit different physical and chemical properties and it is well accepted that the crystalline phase plays an important role in photocatalytic reactions. Anatase is often regarded as the most efficient phase of titania, presumably due to the combined effect of lower recombination rate between the photogenerated charges and higher surface adsorptive capacity that means efficient holes scavenging activity [5-11], but some researchers stated that rutile is the most effective phase [12, 13].

There are several contradictory reports in the literature concerning the effect of mixed crystal phase on the photocatalyst performance. Some authors reported that no photocatalytic synergy between anatase-rutile composites exists both in dense thin films with an increasing percentage of rutile [1], and in commercial TiO_2 Degussa P25 [2, 3]. However, it is becoming apparent that TiO_2 based photocatalysts containing both phases in intimate contact show enhanced photocatalytic activities not assignable to the single phases [4]. This improved activity should be ascribed to longer lifetimes of electrons and holes, which can be spatially separated due to their transfer between the two different phases.

Much confusion is present in the literature as to whether or not electrons are shuttled from anatase to rutile or vice-versa. Some research groups have reported that electrons move from the higher conduction band of anatase to rutile [14-17]. In this regard, based on the transient MIR dynamics of anatase-rutile mixed phase TiO_2, Shen et al. demonstrated recently that charge transfer process from anatase to rutile occurs at the phase junction [16]. On the contrary, other authors claimed that the electron movement can be from rutile to trapping sites of anatase that lie below the rutile conduction band [18-26]. Kullgren et al. using high level electronic structure calculations concluded that, at typical rutile/anatase interfaces, accumulation of mobile electrons in anatase and mobile holes in rutile occurs [23]. A similar kind of charge separation was also reported by Carneiro et al. [24]. Some researchers demonstrated that the conduction band energy increase in the space charge layer of anatase,

caused by UV irradiation of TiO_2 Degussa P25, stops electrons going from anatase to rutile, with holes transferred to rutile [25]. Very recently, other authors have examined closely the band alignment between anatase and rutile demonstrating that electron affinity of anatase is higher than that of rutile [26].

The photocatalytic performance of TiO_2 largely depends on the surface properties. In particular, the nature of the surface phases, which are directly exposed to the UV light source and to reactants, should have a crucial role in photocatalysis since photoinduced reactions take place on the surface and photogenerated electrons and holes might migrate through it. Therefore, investigation on the correlation between surface phases and photoactivity of TiO_2 is of great importance for the building up of new efficient photocatalytic systems. In this regard, it is to mention that phase composition on the surface can be different from that in the bulk. Zhang et al. found that UV Raman spectroscopy is more sensitive to the surface region of TiO_2 than visible Raman spectroscopy and that this technique can be used for investigating the phase composition present on the surface [27, 28].

Mixed phase TiO_2 materials other than commercial P25 [20] are scarcely studied in photoreduction processes and eventual interactions of the different phases during the reactions have not been well explored. In this context, few papers investigate the effect of TiO_2 phase fractions of anatase and brookite on CO_2 photoreduction [29, 30] showing that the bicrystalline TiO_2 is more active than single anatase and brookite phases due to enhanced interfacial charge transfer between the two crystalline forms.

In this work we synthesize TiO_2 samples by a sol-gel procedure varying the rutile and anatase content by calcination at different temperatures according to the known behavior of titania upon thermal treatment. Then, the samples are characterized by XRD, NIR-Raman, UV-Raman, BET, DR-UV-Vis spectroscopy and SEM. Effects of the mixed phases are discussed in relation to the photocatalytic activity of these materials in the deoxygenation of methyl *p*-tolyl sulfoxide. This kind of reaction has been chosen as an example of a reductive process on TiO_2 that has not been widely studied in literature. [31, 32]

2. Experimental.

2.1 Photocatalyst preparation. The samples were prepared following a modified precipitation method reported in literature [27]. Titanium (IV) n-butoxide ($Ti(OBu)_4$, 10 mL) was added to anhydrous ethanol (50 mL). Then, this solution was added dropwise to a mixture of distilled water (40 mL) and ethanol (50 mL). A white precipitate immediately formed. It was kept in suspension by stirring

continuously for 24 hrs at room temperature. After that, the precipitate was filtered, washed several times with water and then with anhydrous ethanol and dried at 80°C for 24 hrs. Finally, the solid was divided into three portions. Each portion was calcined in air at one of the following temperatures: 500, 700 and 850°C for 4 hrs. The obtained photocatalysts were indicated as TiO_2-500, TiO_2-700 and TiO_2-850.

2.2 Characterization. XRD patterns were recorded on Bruker D8 Advance diffractometer with a CuK_α radiation source. Diffraction patterns were collected from 20° to 80° at a speed of 0.08°/s.

NIR- and UV-Raman spectra were recorded on Renishaw inVia Raman microscope spectrometers equipped respectively with a diode laser emitting at 785 nm and a He-Cd laser emitting at 325 nm. Photons scattered by the sample were dispersed, respectively, by a 1200 and 3600 lines/mm grating monochromator and were simultaneously collected on a CCD camera. The laser power was limited in both cases in order not to have sample decomposition. BET measurements were carried out by means of ASAP2020 by Micromeritics using N_2 adsorption at 77K. DR-UV-Vis spectra were collected with a Jasco V-570 spectrophotometer equipped with a diffuse reflectance accessory and using $BaSO_4$ as reference. SEM images were obtained by a Hitachi H-800 instrument.

2.3 Methyl p-tolyl sulfoxide deoxygenation. Solvents, methyl p-tolyl sulfoxide and methyl p-tolyl sulfide were purchased from Sigma-Aldrich and used without further purification. In a typical photocatalytic experiment, the chosen photocatalyst (20 mg) was suspended in a mixture of CH_3CN/2-propanol (4/1 v/v, 3 mL) containing methyl p-tolyl sulfoxide (1.55×10^{-3} M, Sigma Aldrich). The sample was outgassed with a N_2 flux for 30 minutes and then irradiated with a medium pressure Hg lamp (Helios Italquartz Q-400) selecting wavelengths higher than 350 nm with a cut off filter (15 $mWcm^{-2}$). Conversion of sulfoxide to sulfide could be followed by UV-vis analysis. During irradiation, the initial spectrum of sulfoxide decreased (λ_{max} = 240 nm) and only one peak grew (λ_{max}= 254 nm), corresponding to sulfide, as verified from comparison with an authentic sample. Deconvolution of the spectra allows us to build a calibration curve at λ = 254 nm that shows a linear function of absorbance vs. concentration (A=12094C). Furthermore, to confirm UV data, product analyses were also carried out using a HP 6890 gas chromatograph equipped with a flame ionization detector and an HPWAX capillary column (splitless, N_2 carrier, programme temperature: 100°C 15 min, 15°C/min, 160°C 18 min). From GC analysis only one peak was detected whose retention time (15.3 min) corresponded to that of the sulfide authentic sample, confirming UV results. Moreover, we verified that the loss in sulfoxide concentration was equal to the increase of sulfide concentration. Quantitative analyses were

performed using a calibration curve of sulfide (equation was: peak area=1.29x10^{10}C). The values of sulfide concentration obtained from these two independent techniques were in agreement with each other within an experimental error of 10%. Each photocatalytic experiment was repeated three times in order to evaluate the error, which remained in the ± 5% interval around mean value. In order to test the stability of the photocatalysts, the most active TiO_2-700, recovered at the end of the photocatalytic experiment, was washed three times with CH_3CN (1 mL) and then dried overnight in the oven. Finally it was calcined at 400 °C for six hours and used in a subsequent experiment. Control experiments were run irradiating the solution of methyl p-tolyl sulfoxide (1.55 x 10^{-3}M) without any photocatalyst at $\lambda >$ 350 nm or keeping in the dark TiO_2-700 dispersed in the solution containing the sulfoxide. Moreover, we performed other experiments with the aim of optimizing the slurry amount of photocatalyst with respect to absorption of incident light. Twenty milligrams of photocatalyst were chosen as the optimum amount.

3. Results and discussion

3.1 XRD patterns of TiO_2 calcined at different temperatures.

Fig. 1 shows the XRD patterns of TiO_2 before and after calcination at 500, 700 and 850° C. For the sample before calcination, diffraction peaks due to the crystalline phases are not observed, giving evidence that the sample is amorphous. For TiO_2-500, the peak at 25.3° relative to anatase is very intense and narrow and that at 27.4° ascribed to rutile has a very low intensity. These evidences indicate that anatase is the main crystalline phase in this sample, but little percentage of rutile is already present. Increasing calcination temperature to 700°C, the intensity of the anatase peaks decreases and, at the same time, that of rutile increases, indicating that anatase phase is transforming into the rutile one. Going further, TiO_2-850 presents only the diffraction peaks of rutile and those assigned to anatase disappeared. This means that, at this temperature, anatase completely changed to the rutile phase.

The weight fraction of the rutile phase (x_R) can be estimated from the XRD peak intensities using the following formula [33]:

$$x_R = 1/[1+0.884(I_A/I_R)]$$

where I_A and I_R represent the X-ray integrated intensities of anatase (101) and rutile (110) diffraction peaks respectively. Results are reported in Table 1 (first column).

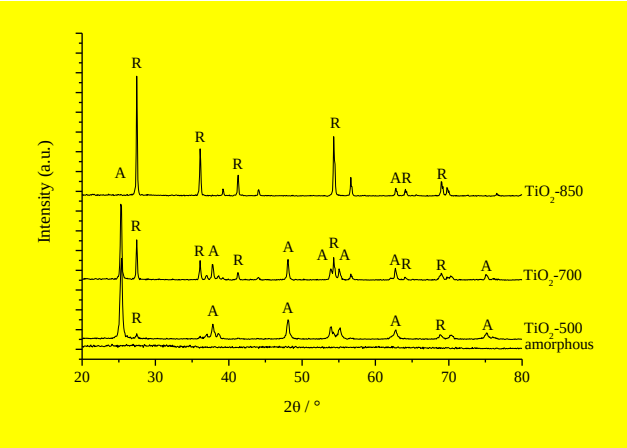

Fig.1 XRD patterns of TiO_2 before calcination and of TiO_2 calcined at different temperatures.

Table 1. Phase composition, crystallite size and surface area of the photocatalysts.

photocatalyst	phase composition from XRD	particles diameter (nm)	BET (m^2/g)
TiO_2-500	93% A, 7% R	50-60	27
TiO_2-700	60% A, 40% R	90-150	20
TiO_2-850	0% A, 100% R	100-150	8

3.2 DR-UV- visible spectra.

Fig. 2A reports DR-UV-vis spectra of the investigated TiO_2 samples. It can be seen that, going from TiO_2-500 to TiO_2-850, the absorption onset shifts to longer wavelengths, in agreement with the increasing amount of rutile, which it is well known to have a band gap value lower than that of anatase. Looking at the first derivative curves (Fig. 2B), we observe a peak centered at 365 nm for TiO_2-500 and a peak at 401 nm for TiO_2-850 that can be ascribed to anatase and rutile respectively, according to literature data [12]. Interestingly, the sample TiO_2-700 presents both peaks, indicating that anatase and rutile are both present in agreement with XRD data.

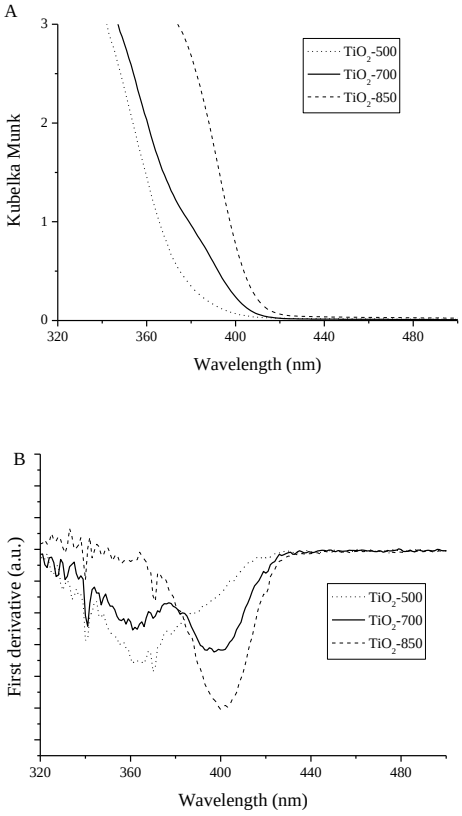

Fig. 2A) DR-UV-vis spectra of TiO_2-500, TiO_2-700 and of TiO_2-850. B) The first derivative curves obtained from part A.

3.3 NIR- and UV-Raman spectra.

Fig. 3 displays the NIR Raman spectra of TiO_2 calcined at different temperatures. In the sample calcined at 500°C characteristic bands of anatase appear at 638, 515, 395 and 195 cm^{-1}. This result is in agreement with XRD data that established that more than 90% was anatase. However, no peak relative to the little amount of rutile has been detected by the Raman spectrum. When the sample is calcined at 700°C the bands of anatase decrease in intensity and other new bands at 612 and 446 cm^{-1} ascribable to rutile phase appear. The simultaneous presence of anatase and rutile confirms the results of XRD and

DR-UV-Vis analyses and the gradual transformation of anatase to rutile by increasing calcination temperature. In fact, TiO_2-850 presents only the bands characteristic of rutile (612, 446, 234 cm^{-1}).

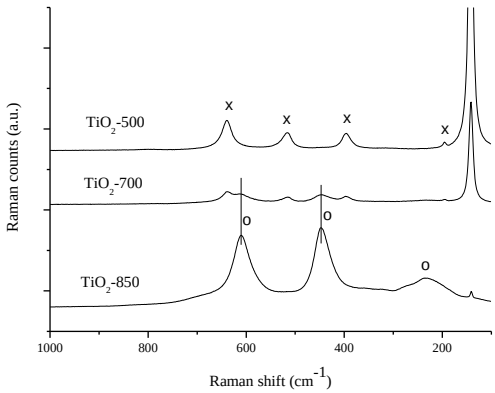

Fig. 3 NIR Raman spectra of TiO_2-500, TiO_2-700 and of TiO_2-850 (λ_{exc}= 785 nm)

Some authors reported recently that, in the case of TiO_2 particles, information from UV Raman can be often different from that obtainable with longer wavelengths [27]. In particular, they distinguish between laser light sources, claiming that signals of Raman spectra recorded upon excitation with short frequency radiation mainly come from the bulk of TiO_2. For this, Raman spectroscopy can be considered a bulk-sensitive method, like XRD [27, 34-37]. Moreover, Zhang et al. report that the use of an UV light source, which has a lower penetration power than longer wavelengths, could contain more signal from the surface skin region than from the bulk of the TiO_2 sample [27, 28]. For our purposes, since we use UV light during the photocatalytic experiments (see below), it is important to establish which phase is present on the TiO_2 surface and, thus, exposed to the photochemical excitation. On this basis, we decided to record UV-Raman spectra of the three samples under investigation (Fig. 4). The quality of the rutile UV Raman spectrum is always lower respect to that of anatase. This is due to resonant effect. For this, it is expected that rutile contribution reveals to be just a shoulder if present when anatase is the main crystal phase. Analogously to what observed in NIR-Raman spectra, TiO_2-850 consists of rutile and TiO_2-500 consists mainly of anatase. The eventual presence of rutile traces on the surface of this sample is below the instrumental detection limit. In the case of TiO_2-700 we clearly observe the peaks characteristic of anatase. A deep analysis of the anatase peak at 638 cm^{-1} (Fig. 4B)

reveals also the presence of rutile phase by the detection of a shoulder at lower wavenumbers. The comparison between NIR-Raman and UV-Raman spectra lets us to conclude that, although anatase phase is persisting on the surface of TiO_2-700 at relatively high calcination temperatures, both phases are present on the surface and can participate to the photocatalytic process.

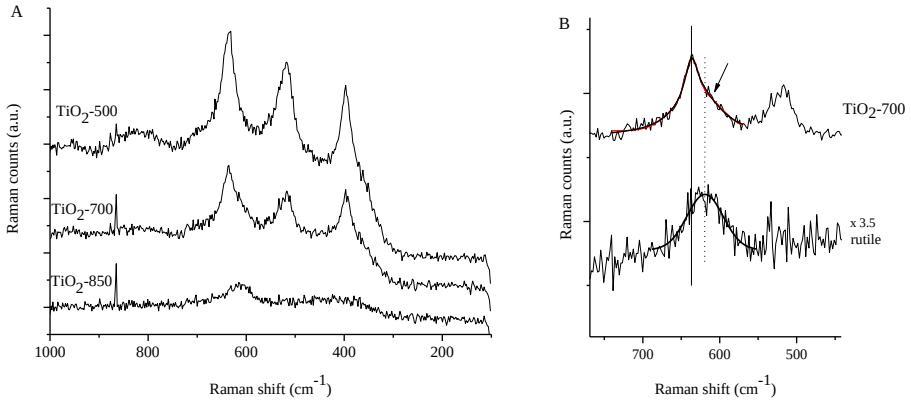

Fig. 4. A) UV-Raman spectra of TiO_2-500, TiO_2-700 and of TiO_2-850 (λ_{exc}= 325 nm). B) Expanded view of the region from 450 to 750 cm^{-1} in TiO_2-700 spectrum of part A and commercial rutile spectrum in the same range of wavenumbers. The intensity of rutile spectrum has been multiplied by 3.5.

3.4 SEM, BET analyses

Specific surface areas and morphology of the three samples have been investigated by N_2 adsorption at 77K and SEM respectively. The values of surface area are reported in Table 1. It is seen that increasing calcination temperature and the content of rutile, the surface area decreases and, at the same time, particle size tends to increase, in agreement with what is reported in the literature [27, 38]. However, as shown in Fig. 5, the increase of particle size is more pronounced passing from TiO_2-500 to TiO_2-700 than from TiO_2-700 to TiO_2-850 (see Table 1).

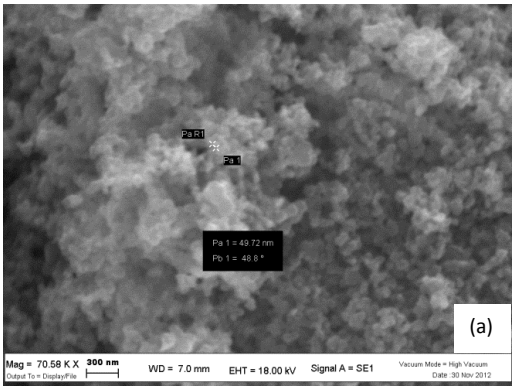
Pa R1
Pa 1
Pa 1 = 49.72 nm
Pb 1 = 48.8 °
(a)
Mag = 70.58 K X
300 nm
WD = 7.0 mm
EHT = 18.00 kV
Signal A = SE1
Vacuum Mode = High Vacuum
Date :30 Nov 2012

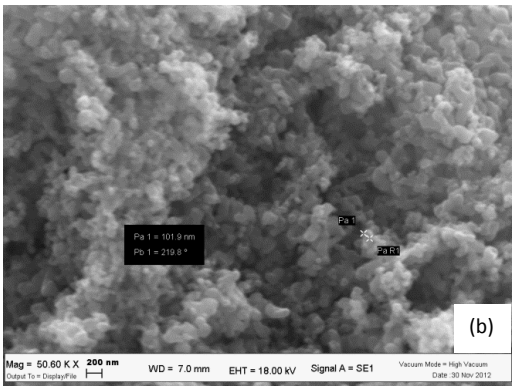
Pa 1
Pa R1
Pa 1 = 101.9 nm
Pb 1 = 219.8 °
(b)
Mag = 50.60 K X
200 nm
WD = 7.0 mm
EHT = 18.00 kV
Signal A = SE1
Vacuum Mode = High Vacuum
Date :30 Nov 2012

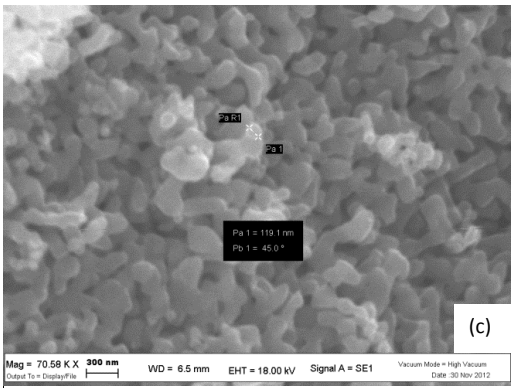
Pa R1
Pa 1
Pa 1 = 119.1 nm
Pb 1 = 45.0 °
(c)
Mag = 70.58 K X
300 nm
WD = 6.5 mm
EHT = 18.00 kV
Signal A = SE1
Vacuum Mode = High Vacuum
Date :30 Nov 2012

Fig. 5 SEM images of TiO_2-500 (a), TiO_2-700 (b) and of TiO_2-850 (c).

3.5 Photocatalytic activity

Irradiation (λ> 350 nm) of deaerated suspensions of the investigated photocatalysts (20 mg) in CH_3CN/2-propanol(4/1 v/v, 3 mL) containing methyl p-tolyl sulfoxide (1.55×10^{-3}M) led to the formation of methyl p-tolyl sulfide (see experimental part). Its formation has been followed during one hour irradiation as shown in Fig. 6. From gas chromatographic analysis and UV spectra we quantified that the decrease of substrate concentration corresponds to the formed product, with a selectivity of 100%. For this, we can claim that no other side products are formed during the deoxygenation reaction. This result is of relevance since other authors reported in the past that irradiation of TiO_2 (Aldrich 99%) dispersed in pure ethanol in the presence of methyl p-tolyl sulfoxide (1.0×10^{-3}M) led to methyl p-tolyl sulfide with a selectivity of only 73%. Moreover, no data have been reported about the phase of the photocatalyst, and the relation between the crystalline phase and the photoactivity has not been considered [31, 32]. In our system 2-propanol scavenges the photogenerated holes [39].

From Fig. 6A we observe that the most active photocatalyst is TiO_2-700, TiO_2-500 follows, and TiO_2-850 shows a very poor photocatalytic activity. Since from Table 1 the three TiO_2 based samples have different surface area values, Fig. 6B reports sulfide concentration values normalized to the effective area present in 20 mg of employed photocatalyst.

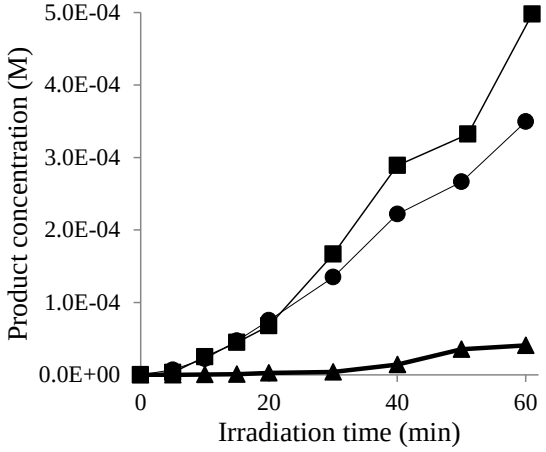

Fig. 6A Methyl p-tolyl sulfide concentration vs. irradiation time obtained upon irradiation of deaerated solutions of CH_3CN/2-propanol (4/1 v/v) containing methyl p-tolyl sulfoxide (1.55×10^{-3}M) as substrate in which the photocatalyst (20 mg) has been dispersed. Squares: TiO_2-700, circles TiO_2-500, triangles TiO_2-850.

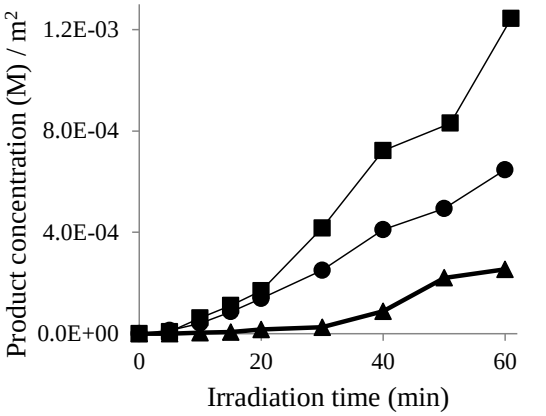

Fig. 6B Methyl p-tolyl sulfide concentration (values from Fig. 7A) / surface area vs. irradiation time. Squares: TiO_2-700 (0.4 m^2), circles TiO_2-500 (0.54 m^2), triangles TiO_2-850 (0.16 m^2).

Fig. 6B shows that TiO_2-500, containing more than 90% of anatase, is more active than TiO_2-850 that is made of rutile. These results are in agreement with the facts that charge recombination process in anatase is known to be relatively slow [6] and that good interaction between anatase and 2-propanol probably occurs, leading to efficient holes scavenging activity [5]. Interestingly, the presence of both anatase and rutile in comparable amount on the surface of TiO_2-700 has an important role in increasing the photocatalytic activity with respect to TiO_2-500 and TiO_2-850. Many literature works report that the efficiency of charges separation process in titania is enhanced when both phases are present [13-26] and our results reinforce this idea. In our photocatalytic system, deoxygenation reaction uses promoted electrons and 2-propanol oxidation needs photogenerated holes. The increase in photocatalytic activity of TiO_2-700 is likely due to spatial separation of electrons and holes on the two different phases, which enhances their lifetime, so increasing the efficiency of reduction and oxidation processes. Two possible mechanisms of charge separation, both supported by literature, can be invoked: the first is the movement of electrons from rutile to anatase and the second is the shuttle of electrons from anatase to rutile (Scheme 1A and 1B respectively). In Scheme 1A it is to consider that UV illumination ($\lambda > 350$ nm) photoexcites both phases: electrons promoted to the conduction band of rutile can flow to anatase thanks to its reported higher electron affinity [26] and, at the same time, photogenerated holes can migrate toward rutile phase [24]. This kind of charge separation is supported also by Sun and coworkers, who suggested that UV irradiation of TiO_2 P25 causes a band bending of 0.1 eV that inhibits the thermodynamically allowed transfer of electrons from anatase to rutile [25]. Looking at Fig. 6B, we observe that photocatalytic activities of TiO_2-500 (anatase) and of TiO_2-700 (mixed phase) are very similar at the initial stages of the experiment and diverge at irradiation times longer than 20 minutes. This behavior could be in agreement with this hypothesis. The electron transfer from rutile to anatase does not mean that the hole transfer process does not proceed in mixed phase TiO_2. Holes could be transferred to rutile and be scanvenged there by 2-propanol. This means that the alcohol should be very important to the effectiveness of the sulfoxide photoreduction reaction over TiO_2. On this regard, it has been reported that calcination treatment of TiO_2 rutile samples leads to a very small surface hydroxyl concentration [24] and that alcohol molecules can be dissociatively adsorbed as alcoholate species [39-41] on these dehydroxylated rutile surfaces. The reaction between adsorbed alcoholate and holes is generally fast and may contribute to the efficiency of the sulfoxide photoreduction.

Scheme 1B proposes the thermodynamically allowed transfer of photoexcited electrons from anatase to rutile [17]. Hole scavenging by 2-propanol would occur mostly on anatase, which is reported to be the most reactive phase with alcohols [5]. An improved photocatalytic reduction reaction efficiency implies both a good charge separation and an efficient process of holes scavenging and these considerations could explain the enhancement of TiO_2-700 photoactivity.

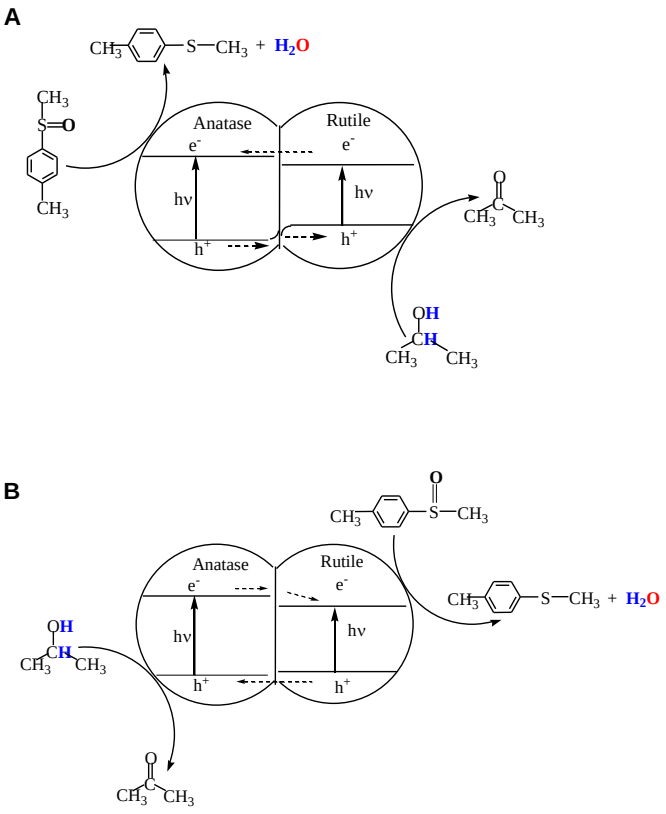

Scheme 1. Possible mechanisms for the deoxygenation of methyl p-tolyl sulfoxide with the TiO_2-700 mixed-phase photocatalyst.

Stability of the photocatalyst has been evaluated for the most active TiO_2-700. At the end of the photocatalytic experiment, the material is recovered and treated as described in the experimental part. It

is found that calcination is a necessary step to recover the photocatalytic activity. Three repeated experiments show that it can be re-used with good results (Fig. 7). We observe a loss of photocatalytic activity, in terms of formed end product, between the first and the second run of about 20% but no significant decrease is seen between the second and the third run.

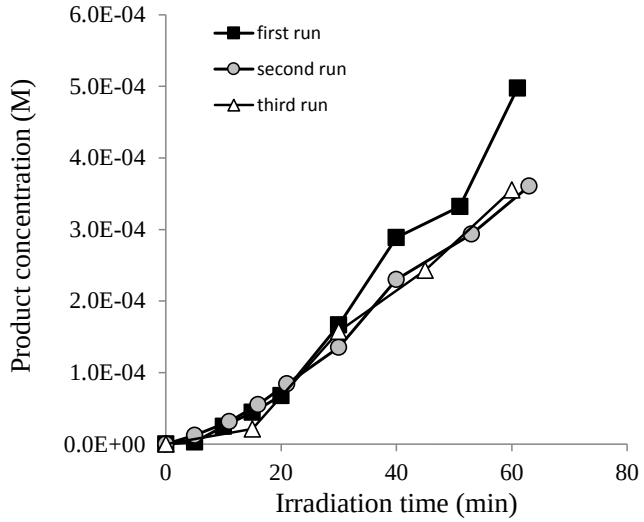

Fig. 7 Methyl p-tolyl sulphide concentration vs. time upon irradiation of TiO_2-700 in three repeated cycles.

Conclusions

Anatase and rutile formation has been thermally induced calcinating at different temperatures amorphous TiO_2 prepared by a sol-gel method. Three photocatalysts have been synthesized and fully characterized. Then, they have been tested in the deoxygenation of methyl p-tolyl sulfoxide to the corresponding sulfide. UV- Raman spectrum of TiO_2-700 (calcined at 700°C) shows that anatase and rutile are both present on the surface. Their presence is responsible of the improvement of photocatalytic activity with respect to single phases. This positive performance is attributed to a synergy between anatase and rutile that allows an efficient charges separation process with electrons and holes on the two different phases. This work points out that a suitable surface composition of TiO_2

together with a good holes scavenger produces a more efficient photocatalyst, useful in processes of synthetic interest. We underline that the conversion of the sulfoxide to sulfide is completely selective under the used reaction conditions. Research is going on both in the preparation of other photocatalysts with intermediate anatase-rutile ratios on the surface and in the comprehension of the details of charges movement.

Acknowledgement. We kindly acknowledge Gabriele Bertocchi for XRD analysis, and Daniela Palmeri for SEM images. We are also grateful to the University of Ferrara (Fondi FAR) and to the University of Torino (FIRB RBAP115AYN) for the financial support.

References

[1] K. Nagaveni, G. Sivalingam, M. S. Hedge, G. Madras, Appl. Catal. B 48 (2004) 83-93.

[2] A. L. Linsebigler, G. Q. Lu, J. T. Yates, Chem. Rev. 95 (1995) 735-758.

[3] M. R. Hoffmann, S. T. Martin, W. Y. Choi, D. W. Bahnemann, Chem. Rev. 95 (1995) 69-96.

[4] T. Ohno, K. Sarukawa, M. Matsumara J. Phys. Chem. B 105 (2001) 2417-2420.

[5] A. Y. Ahmed, T. A. Kandiel, T. Oekermann, D. Bahnemann, J. Phys. Chem. Lett. 2 (2011) 2461-2465.

[6] C. Colbeau-Justin, M. Kunst, D. Huguenin, J. Mater. Sci. 38 (2003) 2429-2437.

[7] T. Luttrell, S. Halpegamage, J. Tao, A. Kramer, E. Sutter, M. Batzill, Scientific Reports, 2014, 4 article n° 4043.

[8]Y. Shiraishi, Y. Togawa, D. Tsukamoto, S. Tanaka, T. Hirai, ACS Catal. 2 (2012) 2475-2481.

[9] Y. Shiraishi, H. Hirakawa, Y. Togawa, Y. Sugano, S. Ichikawa, T. Hirai, ACS Catal. 3 (2013) 2318-2326.

[10] A. Kafizas, C. J. Carmalt, I. P. Parkin, Chem. Eur. J. 18 (2012) 13048-13058.

[11] B. Ohtani, O. O. Prieto-Mahaney, D. Li, R. Abe, J. Photochem. Photobiol. A: Chem. 216 (2010) 179-182.

[12] P. Apopei, C. Catrinescu, C. Teodosiu, S. Royer, App. Catal. B: Environ. 160-161 (2014) 374-382.

[13] M. A. Henderson, Surf. Sci. Reports 66 (2011) 185-297 and references therein.

[14] M. Yan, F. Chen, J. Zhang, M. Anpo, J. Phys. Chem. B 109 (2005) 8673-8678.

[15] D. Jiang, S. Zhang, H. Zhao, Environ. Sci. Technol. 41 (2007) 303-308.

[16] J. Yu, J. C. Yu, W. Ho, Z. Jiang, New J. Chem. 26 (2002) 607-613.

Formattato: Italiano (Italia)

[17] S. Shen, X. Wang, T. Chen, Z. Feng, C. Li, J. Phys. Chem. C 118 (2014) 12661-12668.
[18] D. C. Hurum, A. G. Agrios, K. A. Gray, T. Rajh, M. C. Thurnauer, J. Phys. Chem. B 107 (2003) 4545-4549.
[19] C. A. Emilio, M. I. Litter, M. Kunst, M. Bouchard, C. Colbeau-Justin, Langmuir 22 (2006) 3606-3613.
[20] G. Li, S. Ciston, Z. V. Saponjic, L. Chen, N. M. Dimitrijevic, T. Rajh, K. A. Gray, J. Catal. 253 (2008) 105-110.
[21] T. Ohno, K. Tokieda, S. Higashida, M. Matsumura, Appl. Catal. A: General 244 (2003) 383-391.
[22] G. Li, L. Chen, M. E. Graham, K. A. Gray, J. Mol. Catal. A: Chem. 275 (2007) 30-35.
[23] J. Kullgren, H. A. Huy, B. Aradi, T. Frauenheim, P. Deak, Phys. Status Solid RRL 8 (2014) 566-570.
[24] J. T.Carneiro, T. J. Savenije, J. A. Moulijn, G. Mul, J. Phys. Chem. C 115 (2011) 2211-2217.
[25] B. Sun, A. V. Vorontsov, P. G. Smirniotis, Langmuir 19 (2003) 3151-3156.
[26] D. O. Scanlon, C. W. Dunnill, J. Buckeridge, S. A. Shevlin, A. J. Logsdail, S. M. Woodley, C. R. A. Catlow, M. J. Powell, R. G. Palgrave, I. P. Parkin, G. W. Watson, T. W. Keal, P. Sherwood, A. Walsh, A. A Sokol, Nature Mater. 12 (2013) 798-801.
[27] J. Zhang, M. Li, Z. Feng, J. Chen, C. Li, J. Phys. Chem. B 110 (2006) 927-935.
[28] J. Zhang, Q. Xu, Z. Feng, M. Li, C. Li, Angew. Chem. Int. Ed. 47 (2008) 1766-1769.
[29] H. Zhao, L. Liu, J. M. Andino, Y. Li, J. Mater. Chem. A 1 (2013) 8209-8216.
[30] L. Liu, H. Zhao, J. M. Andino, Y. Li, ACS Catal., 2012, 2, 1817-1828.
[31] C. Srinivasan, Curr. Sci. 76 (1999) 534-539.
[32] N. Somasundaram, K. Pitchumani, C. Srinivasan, J. Chem. Soc. Chem. Comm. (1994) 1473.
[33] A. A. Gribb, J. F. Banfield, Am. Mineral. 82 (1997) 717-728.
[34] T. D. Robert, L. D. Laude, V. M. Geskin, R. Lazzaroni, R. Gouttebaron, Thin Solid Films, 2003, 440, 268-277.
[35] A. Welte, C. Waldauf, C. Brabec, P. J. Wellmann, Thin Solid Films, 2008, 516, 7256-7259.
[36] S. Kambe, S. Nakade, Y. Wada, T. Kitamura, S. Yanagida, J. Mater. Chem., 2002, 12, 723-728.
[37] M. S. P. Francisco, V. R. Mastelaro, Chem. Mater., 2002, 14, 2514-2518.
[38] K.N.P. Kumar, K. Keizer, A.J. Burggraaf, T. Okubo, H. Nagamoto, S. Morooka, Nature 358 (1992) 48-51.
[39] A. Molinari, A. Maldotti, R. Amadelli, Curr. Org. Chem., 2013, 17, 2382-2405 and references therein.

Formattato: Italiano (Italia)

[40] Y. Suda, T. Morimoto, M. Nagao, Langmuir 3 (1987) 99-104.
[41] V. Augugliaro, T. Caronna, V. Loddo, G. Marcì, G. Palmisano, L. Palmisano, S. Yurdakal, Chem. Eur. J. 14 (2008) 4640-4646.